

Determination of S_{17} from ${}^8\text{B}$ breakup by means of the method of continuum-discretized coupled-channels

K. Ogata,^{1,*} S. Hashimoto,¹ Y. Iseri,² M. Kamimura,¹ and M. Yahiro¹

¹*Department of Physics, Kyushu University, Fukuoka 812-8581, Japan*

²*Department of Physics, Chiba-Keizai College, Todoroki-cho 4-3-30, Inage, Chiba 263-0021, Japan*

(Dated: February 9, 2020)

The astrophysical factor for ${}^7\text{Be}(p, \gamma){}^8\text{B}$ at zero energy, $S_{17}(0)$, is determined from ${}^{208}\text{Pb}({}^8\text{B}, p+{}^7\text{Be}){}^{208}\text{Pb}$ at 52 MeV/nucleon. We use the method of continuum-discretized coupled-channels (CDCC) to accurately calculate the ${}^8\text{B}$ breakup cross section, taking account of nuclear breakup, Coulomb dipole and quadrupole transitions and higher-order processes. The asymptotic normalization coefficient (ANC) method is used to extract $S_{17}(0)$ from the calculated breakup-cross-section. The main result of the present paper is $S_{17}(0) = 20.9_{-1.9}^{+2.0}$ eV b. This result has $+4.5\%/ -2.6\%$ theoretical error, which comes from ambiguity of the p - ${}^7\text{Be}$ scattering length, and 8.4% systematic experimental error. CDCC calculation with one-step Coulomb dipole transitions results in a smaller value of $S_{17}(0)$, $19.0_{-1.7}^{+1.9}$ eV b, which agrees well with the extracted value with the first-order perturbation theory: 18.9 ± 1.8 eV b. Inclusion of Coulomb quadrupole transitions in one-step CDCC calculation is found to give further reduction of $S_{17}(0)$. Multistep processes give about 20% contribution to $S_{17}(0)$ in the present case. The analysis with the ANC method is also applied to direct measurement of ${}^7\text{Be}(p, \gamma){}^8\text{B}$ and $S_{17}(0) = 21.7_{-0.55}^{+0.62}$ eV b is obtained, which is consistent with the result of precise measurement of the p -capture reaction: $S_{17}(0) = 22.1 \pm 0.6$ (expt) ± 0.6 (theo) eV b. Thus, the discrepancy between the values of $S_{17}(0)$ obtained from direct ${}^7\text{Be}(p, \gamma){}^8\text{B}$ and indirect ${}^8\text{B}$ -breakup measurements is essentially removed.

PACS numbers: 24.10.Eq, 25.60.Gc, 25.70.De, 26.65.+t

I. INTRODUCTION

The solar neutrino problem is one of central issues in the neutrino physics [1]. The current interpretation of the solar-neutrino deficit is the neutrino oscillation induced by the mass difference among ν_e , ν_μ and ν_τ , and their mixing angles [2]. Then, attention is now focused on determining the oscillation parameters with observations. The astrophysical factor $S_{17}(E)$, defined by $S_{17}(E) = \sigma_{p\gamma}(E)E \exp[2\pi\eta]$ with $\sigma_{p\gamma}$ the cross section of the p -capture reaction ${}^7\text{Be}(p, \gamma){}^8\text{B}$ and η the Sommerfeld parameter, plays an essential role in the solar-neutrino oscillation phenomenology, in the sense that the prediction value for the flux of ${}^8\text{B}$ neutrino, which is intensively detected on the earth, is proportional to the zero incident-energy limit of $S_{17}(E)$, i.e. $S_{17}(0)$. The required accuracy for $S_{17}(0)$ from astrophysics is about 5% in errors [3].

Recently, precise measurement of $\sigma_{p\gamma}(E)$, i.e. $S_{17}(E)$, has been carried out by Junghans *et al.* [4] at energies of $E = 116$ – 2460 keV, which are rather small but still higher than stellar energies (~ 20 keV), and $S_{17}(0) = 22.1 \pm 0.6$ (expt) ± 0.6 (theo) eV b was derived by extrapolating the measured $S_{17}(E)$ to the zero incident-energy limit with a three-cluster model [5] for ${}^8\text{B}$ structure. However, this extrapolation is still ambiguous, since the three-cluster model does not reproduce the measured $S_{17}(E)$ sufficiently in both magnitude and E -dependence. Moreover, as pointed out in Ref. [6], uncertainty of the p - ${}^7\text{Be}$ scattering length (about 50% in error) prevents one from determining $S_{17}(0)$ with very high accuracy.

Because of difficulties of the direct measurement at stellar energies, alternative indirect measurements were proposed.

Coulomb dissociation [7, 8, 9, 10, 11, 12, 13] of ${}^8\text{B}$ is one of such indirect measurements. So far extraction of $S_{17}(0)$ from these experiments was based on the virtual photon theory, which assumes that the ${}^8\text{B}$ is dissociated through its one-step Coulomb dipole (E1) transitions, i.e., with no multistep E1 transitions, no nuclear breakup and no Coulomb quadrupole (E2) transitions. In the analysis of the MSU experiment [12, 13] measured at 44 and 83 MeV/nucleon, exceptionally, the E2 contribution estimated from the parallel-momentum-distribution of ${}^7\text{Be}$ fragment was subtracted from the breakup spectrum of ${}^8\text{B}$. As a result, the extracted $S_{17}(0)$ is $17.8_{-1.2}^{+1.4}$ eV b, which is somewhat smaller than that obtained from the RIKEN experiment, $S_{17}(0) = 18.9 \pm 1.8$ eV b [9]. However, the analysis of the angular distribution of the ${}^8\text{B}$ breakup cross section of the RIKEN experiment at 52 MeV/nucleon showed no contribution of the E2 transitions. Moreover, the recent experiment at rather high energy, 250 MeV/nucleon, done at GSI [11] showed that the E2 contribution is negligibly small; the resulting $S_{17}(0)$ is $18.6 \pm 1.2 \pm 1.0$ eV b. Even though the significance of E2 transitions can be energy-dependent, the conclusions of the MSU and RIKEN measurements at similar energies are clearly inconsistent and roles of the E2 component are still under discussion. More seriously, there exists a non-negligible discrepancy of about 15% between the values of $S_{17}(0)$ derived from direct p -capture and indirect ${}^8\text{B}$ -breakup measurements.

Very recently, it was shown by semiclassical calculation of ${}^{208}\text{Pb}({}^8\text{B}, p+{}^7\text{Be}){}^{208}\text{Pb}$ at 52 MeV/nucleon that the discrepancy mentioned above was significantly reduced by the inclusion of nuclear-breakup components, E2 transitions and higher-order processes [14]. Motivated by this result, in the present paper we attempt to extract a reliable value of $S_{17}(0)$ from ${}^8\text{B}$ dissociation experiment measured at RIKEN [7, 8, 9], with a sophisticated method with three-body reaction

*Electronic address: kazu2scp@mbox.nc.kyushu-u.ac.jp

model, that is, the method of continuum-discretized coupled-channels [15, 16] (CDCC). CDCC was shown to describe various processes where effects of projectile-breakup are essential [17, 18, 19, 20, 21, 22, 23, 24, 25], and it has also been applied to ^8B nuclear and Coulomb breakup with high degrees of success [13, 26, 27, 28].

In order to extract $S_{17}(0)$ from the result of the CDCC analysis of ^8B breakup based on the $p+^7\text{Be}+\text{A}$ three-body model, we use the asymptotic normalization coefficient (ANC) method [29, 30], which accurately determines $S_{17}(0)$ if the tail of the ^8B wave function is well determined. As important advantage of the use of the ANC method, the reaction mechanism is not restricted; namely, nuclear breakup, E2 transitions and higher-order processes can all be included in the analysis. Additionally, the uncertainty of $S_{17}(0)$ coming from the use of the ANC method can quantitatively be evaluated, as mentioned in Refs. [25, 28].

The purpose of the present paper is as follows. First, we describe how to extract the ANC from the CDCC analysis of ^8B breakup. The CDCC wave function contains not only the ground state of ^8B but also its continuum states and includes all higher-order processes. So it is not trivial that the breakup cross section obtained with CDCC σ_{CDCC} is proportional to the spectroscopic factor $\mathfrak{S}_{\text{exp}}$ that shows the incompleteness of the $p+^7\text{Be}$ two-body picture for the *ground state* of ^8B . We show a condition that makes $\sigma_{\text{CDCC}} \propto \mathfrak{S}_{\text{exp}}$ and estimate angular region of ^8B breakup where the ANC analysis with CDCC works. Second, we determine $S_{17}(0)$ from $^{208}\text{Pb}(^8\text{B}, p+^7\text{Be})^{208}\text{Pb}$ at 52 MeV/nucleon by the ANC method, taking account of nuclear and Coulomb breakup and all higher-order processes. It should be noted that in our CDCC calculation interference between nuclear- and Coulomb-breakup amplitudes is explicitly included. In numerical calculation we make use of the eikonal-CDCC method (E-CDCC) [31], with some modifications, to obtain the scattering amplitude corresponding to large values of the orbital-angular-momentum L between the projectile and the target nucleus. We then construct a hybrid amplitude from the results of E-CDCC and CDCC. This method allows one to make very accurate analysis of nuclear and Coulomb breakup of ^8B with high computational speed [31]. Uncertainties of the extracted $S_{17}(0)$ from the ^8B breakup by means of CDCC and the ANC method are carefully evaluated. Finally, we discuss the extracted value of $S_{17}(0)$ from the viewpoint of contributions of E2 transitions and higher-order processes. The ANC method is also applied to direct $^7\text{Be}(p, \gamma)^8\text{B}$ measurement and the difference between the values of $S_{17}(0)$ derived from direct and indirect measurements is evaluated.

In Sec. IIA the ANC method is briefly reviewed and in Sec. IIB we describe how to extract the ANC from the CDCC analysis of ^8B breakup. Formulation of modified E-CDCC and construction of the hybrid scattering amplitude are described in Sec. IIC. We describe the numerical inputs in Sec. IIC. We analyze in Sec. IIIB the ^8B breakup cross section measured at RIKEN with CDCC and extract $S_{17}(0)$ by the ANC method. In Sec. IIIC uncertainties of the extracted $S_{17}(0)$ are quantitatively evaluated. The value of the extracted $S_{17}(0)$ is then discussed and compared with that ob-

tained by the virtual photon theory in Sec. IIID. Roles of E2 transitions and higher-order processes are also discussed and the ANC method is applied to precise direct measurement of $^7\text{Be}(p, \gamma)^8\text{B}$. Finally summary and conclusions are given in Sec. IV.

II. FORMALISM

A. The ANC method

Let us consider the radiative capture reaction $p+^7\text{Be} \rightarrow ^8\text{B} + \gamma$ in the low incident-energy limit. The reaction is then dominated by the Coulomb dipole (E1) transitions and is quite peripheral, since the E1 operator suppresses a contribution of the inner part of the ^8B wave function to the cross section $\sigma_{p\gamma}(E)$. The reaction is thus determined only by the tail of the ^8B wave function in the ground state, $\phi_8^{(0)}$. Outside the range R_N of nuclear force working between p and ^7Be , which turned out to be about 4 fm, the overlap function $\varphi_8^{(0)}(r)$ has a simple form, i.e.

$$\begin{aligned} \varphi_8^{(0)}(r) &\equiv \langle \phi_7^{(0)}(\xi_7) | \phi_8^{(0)}(\xi_7, \mathbf{r}) \rangle_{\xi_7, \hat{\mathbf{r}}} \\ &\approx CW_{-\eta, \ell+1/2}(2k_0 r)/r, \quad r > R_N, \end{aligned} \quad (1)$$

where $\phi_7^{(0)}$ is the ground state of ^7Be , k_0 is the relative wave-number between p and ^7Be , and ξ_7 is the internal coordinates of the seven-nucleon system. Moreover, $W_{-\eta, \ell+1/2}$ is the Whittaker function with ℓ the orbital angular momentum between p and ^7Be in the ground state of ^8B ; $\ell = 1$ in the present case. The constant C in Eq. (2) is precisely the ANC that we focus on. One can find that the cross section $\sigma_{p\gamma}(0)$, or $S_{17}(0)$, is proportional to C^2 , by taking the matrix elements of E1 transitions with the use of Eq. (2). Xu *et al.* [30] found that the proportionality constant $S_{17}(0)/C^2$ is 1/0.026. In the present paper we take account of small but non-negligible dependence of $S_{17}(0)/C^2$ on scattering wave-functions between p and ^7Be used in analysis. Following Baye [32], we use the formula

$$S_{17}(0) \approx 38.0(1 - 0.0013\bar{a}_s)C^2, \quad (2)$$

where \bar{a}_s is the p - ^7Be scattering length.

It is possible to determine the ANC from similar reactions involving the overlap function $\langle \phi_7^{(0)}(\xi_7) | \phi_8^{(0)}(\xi_7, \mathbf{r}) \rangle_{\xi_7, \hat{\mathbf{r}}}$, if the reaction is peripheral, namely, the inner part of the ^8B wave function has no contribution. When experimental data are available on such a reaction, the ANC is given by

$$\frac{C^2}{\alpha^2} = \frac{\sigma_{\text{exp}}}{\sigma_{\text{calc}}} \equiv \mathfrak{S}_{\text{exp}}, \quad (3)$$

where σ_{exp} (σ_{calc}) is the experimental (theoretical) cross section. In the calculation of σ_{calc} the unknown overlap function $\varphi_8^{(0)}(r)$ is replaced by a normalized single-particle wave function $f_0(r)$. The constant α in Eq. (3) is the ratio of $f_0(r)$ to $W_{-\eta, \ell+1/2}(2k_0 r)/r$ in the tail region, i.e. the single particle

ANC. Thus, $S_{17}(0)$ can be extracted from indirect measurements. Justification of the use of Eq. (3) in CDCC analysis is described in the next subsection in detail.

It should be noted that we do not care the agreement between $f_0(r)$ and $\varphi_8^{(0)}(r)$ in the inner region, i.e. $r < R_N$. As a result, the spectroscopic factor $\mathfrak{S}_{\text{exp}}$ in Eq. (3) has quite strong dependence on the choice of the ${}^8\text{B}$ single-particle wave function $f_0(r)$. In fact, the ANC method is not suitable for deriving a physically-meaningful $\mathfrak{S}_{\text{exp}}$, since $\mathfrak{S}_{\text{exp}}$, by definition, contains all information of the inner part of the overlap function. On the contrary, the ANC C in Eq. (3) is a physical quantity if the reaction concerned is peripheral, thus it should be determined uniquely. As shown in Sec. III C, $\mathfrak{S}_{\text{exp}}$ and α depend on the single-particle wave function taken, but C hardly depends on it. Consequently, a cross section at extremely low energies can indirectly determined with high accuracy; this prescription is called the ANC method [29].

The ANC method thus designed was originally proposed for p -transfer reactions and actually applied to ${}^{10}\text{Be}({}^7\text{Be}, {}^8\text{B}){}^9\text{Be}$ [33], ${}^{14}\text{N}({}^7\text{Be}, {}^8\text{B}){}^{13}\text{C}$ [34], and ${}^7\text{Be}(d, n){}^8\text{B}$ [25]. In the present paper, alternatively, we aim to extract the ANC from ${}^8\text{B}$ dissociation by ${}^{208}\text{Pb}$ target at intermediate energies. For forward-scattering of ${}^8\text{B}$, the dissociation process is obviously peripheral with respect to R , the relative coordinate between ${}^8\text{B}$ and ${}^{208}\text{Pb}$ (see Fig. 1), from the viewpoint of the classical trajectory. However, peripherality concerned with r , which is an essential condition required by the ANC method, is not obvious and needs to be examined. It should be noted that in our analysis we never assume *a priori* that ${}^8\text{B}$ dissociation is described by the E1 transitions of ${}^8\text{B}$, to which the inner part of the ${}^8\text{B}$ wave function hardly contributes. Quantitative estimation of the accuracy of the ANC method in the present case is done in Sec. III C.

B. Extraction of ANC from ${}^8\text{B}$ breakup

In the present paper, we analyze ${}^8\text{B}$ breakup with CDCC based on the $p+{}^7\text{Be}+A$ three-body model, as in the previous studies [13, 26, 27, 28], and aim at extracting $S_{17}(0)$ with the ANC method. In order to determine C by Eq. (3), however, it must be shown that the cross section σ_{calc} calculated by CDCC is proportional to $\mathfrak{S}_{\text{exp}}$, which is quite nontrivial as mentioned in Sec. I. For this purpose, we start with the $p+{}^3\text{He}+{}^4\text{He}+A$ four-body model illustrated in Fig. 1. Then, with introducing $\mathfrak{S}_{\text{exp}}$, we reduce it to the $p+{}^7\text{Be}+A$ three-body model, on which the actual CDCC calculation is based.

Let us consider A as a heavy target just for simplicity. The triple differential cross section for $({}^8\text{B}, {}^7\text{Be}+p)$ reaction is obtained by $\mathcal{C}\rho|\mathfrak{T}|^2$ with a given factor \mathcal{C} and the three-body phase space factor ρ [35]. The transition amplitude for ${}^8\text{B}$ breakup is

$$\mathfrak{T} = \langle \chi_1 \chi_7 \phi_7^{(0)} | U_{A3} + U_{A4} + U_{A1} + V_{13} + V_{14} | \Psi_{4\text{-body}} \rangle, \quad (4)$$

where χ_1 (χ_7) is the plane wave of outgoing p (${}^7\text{Be}$) relative to A and $\Psi_{4\text{-body}}$ the total (four-body) wave function in the

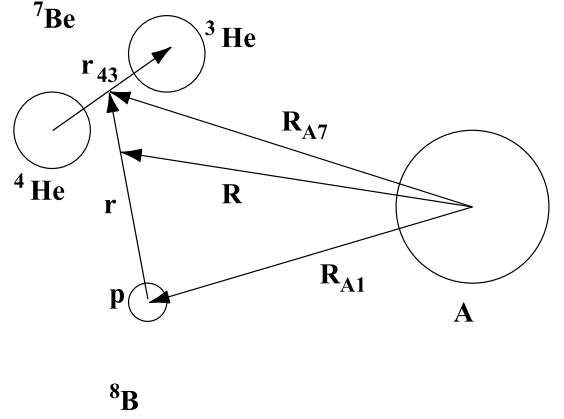


FIG. 1: Illustration of the $p+{}^3\text{He}+{}^4\text{He}+A$ four-body system. Here A is a target.

initial channel. Moreover, U_{XY} (V_{XY}) is the optical potential (two-body interaction) between two nuclei X and Y and the subscripts 1, 3, 4 and A represent p , ${}^3\text{He}$, ${}^4\text{He}$ and A , respectively.

We here assume that ${}^7\text{Be}$ is an inert during the breakup process of ${}^8\text{B}$, which is expected to be valid for forward scattering. In fact, we have confirmed by a ${}^3\text{He}+{}^4\text{He}+{}^{208}\text{Pb}$ three-body model calculation with CDCC that breakup cross sections of ${}^7\text{Be}$ at intermediate energies are less than about 1% of the elastic cross section for $\theta_7 \lesssim 4^\circ$, where θ_7 is the scattering angle of the center-of-mass (c.m.) of ${}^7\text{Be}$. In general θ_7 can differ from the ${}^8\text{B}$ scattering angle θ_8 in the ${}^8\text{B}+{}^{208}\text{Pb} \rightarrow p+{}^7\text{Be}+{}^{208}\text{Pb}$ process. However, the difference between the two angles is very small, since the energy transfer in the ${}^8\text{B}$ breakup concerned here is much smaller than the incident energy of ${}^8\text{B}$.

Thus, for forward scattering of ${}^8\text{B}$, one can replace $U_{A3} + U_{A4}$ in \mathfrak{T} by the single-folding potential $U_{A7} \equiv \langle \phi_7^{(0)} | U_{A3} + U_{A4} | \phi_7^{(0)} \rangle$. Similarly, $V_{13} + V_{14}$ can be replaced by $V_{17} \equiv \langle \phi_7^{(0)} | V_{13} + V_{14} | \phi_7^{(0)} \rangle$. As a result of the replacement, \mathfrak{T} contains the overlap

$$\begin{aligned} \langle \phi_7^{(0)} | \Psi_{4\text{-body}} \rangle &= \langle \phi_7^{(0)} | \frac{i\varepsilon}{E - H_{4\text{-body}} + i\varepsilon} | \phi_8^{(0)} \rangle e^{i\mathbf{P}\cdot\mathbf{R}} \\ &\approx \frac{i\varepsilon}{E - e_7 - H_{3\text{-body}} + i\varepsilon} | \mathfrak{S}_{\text{exp}}^{1/2} \psi_{17}(\mathbf{r}) e^{i\mathbf{P}\cdot\mathbf{R}} \rangle, \end{aligned} \quad (5)$$

where \mathbf{P} is the momentum being conjugate to \mathbf{R} and $H_{4\text{-body}}$ represents the Hamiltonian of the four-body system. In Eq. (5) $\mathfrak{S}_{\text{exp}}^{1/2} \psi_{17}(\mathbf{r}) \equiv \langle \phi_7^{(0)}(\mathbf{r}_{43}) | \phi_8^{(0)}(\mathbf{r}_{43}, \mathbf{r}) \rangle$, namely, $\psi_{17}(\mathbf{r})$ stands for the normalized wave function between ${}^7\text{Be}$ and p in ${}^8\text{B}$, where both ${}^7\text{Be}$ and ${}^8\text{B}$ are in the ground states. The constant $\mathfrak{S}_{\text{exp}}$ is nothing but the spectroscopic factor that means the incompleteness of the two-body ($p+{}^7\text{Be}$) picture for $\phi_8^{(0)}$. Moreover, e_7 is the eigenenergy of $\phi_7^{(0)}$ and $H_{3\text{-body}}$ is the three-body Hamiltonian defined by

$$H_{3\text{-body}} = T_r + T_R + V_{17}(\mathbf{r}) + U_{A7}(\mathbf{R}_{A7}) + U_{A1}(\mathbf{R}_{A1}), \quad (6)$$

where T_r and T_R show the kinetic-energy operators concerned with \mathbf{r} and \mathbf{R} , respectively. Inserting the approximate form of $\langle \phi_7^{(0)} | \Phi_{4\text{-body}} \rangle$ into Eq. (4) leads to

$$\begin{aligned} \mathfrak{T} &\approx \mathfrak{S}_{\text{exp}}^{1/2} \mathfrak{T}_{3\text{-body}}, \\ \mathfrak{T}_{3\text{-body}} &\equiv \langle \chi_1 \chi_7 | U_{A7} + U_{A1} + V_{17} | \Psi_{3\text{-body}} \rangle, \end{aligned} \quad (7)$$

where the three-body wave function $\Psi_{3\text{-body}}$ is a solution of the Schrödinger equation $(H_{3\text{-body}} + e_7 - E) | \Psi_{3\text{-body}} \rangle = 0$. Here E is the total energy of the four-body system that is related to the c.m. incident energy of ${}^8\text{B}$, E_{in} , with $E = E_{\text{in}} + e_7 + e_8$; e_8 is the eigenenergy of the ground state of ${}^8\text{B}$, i.e. -137 keV. The transition amplitude $\mathfrak{T}_{3\text{-body}}$ based on the three-body model is accurately obtained with CDCC [15, 16].

In actual CDCC calculation, the single-folding potential $U_{A7} = \langle \phi_7^{(0)} | U_{A3} + U_{A4} | \phi_7^{(0)} \rangle$ is replaced by the optical potential between A and ${}^7\text{Be}$. Meanwhile, $V_{17} = \langle \phi_7^{(0)} | V_{13} + V_{14} | \phi_7^{(0)} \rangle$ is not uniquely determined yet. However, this is not a problem in the present ANC analysis, because the C extracted from ${}^8\text{B}$ breakup is insensitive to the detail of V_{17} , as shown in Sec. III C.

We have shown above that the cross section calculated by CDCC is indeed proportional to $\mathfrak{S}_{\text{exp}}$, if one concentrates on the forward scattering of ${}^8\text{B}$, say, $\theta_8 \lesssim 4^\circ$. Thus, by using Eq. (3), one can accurately determine C , hence $S_{17}(0)$.

C. E-CDCC and hybrid scattering amplitude

In this subsection we describe the formalism of E-CDCC and how to construct a hybrid scattering-amplitude from the results of E-CDCC and fully quantum-mechanical CDCC. The following formulation contains two important extensions of E-CDCC. One is the inclusion of the intrinsic spin of the projectile and the other is more accurate treatment of the Coulomb wave function in coupled-channel equations than in the previous formulation of E-CDCC [31]. Detailed formalism of CDCC and its theoretical foundation are shown elsewhere [15, 16, 36].

We start with the three-body model shown in Fig. 2 to describe ${}^8\text{B}$ breakup. As already mentioned in Sec. II B, the total

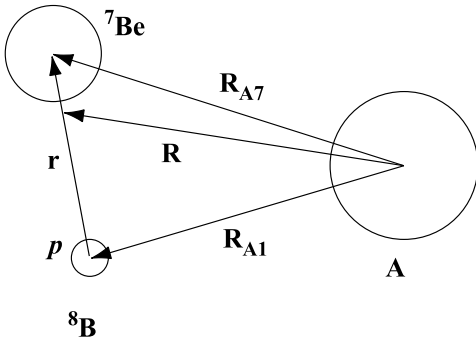


FIG. 2: Illustration of the $p+{}^7\text{Be}+A$ three-body system.

wave function $\Psi_{3\text{-body}}$ satisfies the three-body Schrödinger equation,

$$(H_{3\text{-body}} - E_{\text{in}} - e_8) \Psi_{3\text{-body}}(\mathbf{R}, \mathbf{r}) = 0. \quad (8)$$

We first expand $\Psi_{3\text{-body}}$ in terms of intrinsic wave-functions $\Phi_{i,\ell SI m}(\mathbf{r})$ of ${}^8\text{B}$:

$$\begin{aligned} \Psi_{3\text{-body}}(\mathbf{R}, \mathbf{r}) &= \sum_{i\ell SI m} \Phi_{i,\ell SI m}(\mathbf{r}) \\ &\times \sum_J e^{-i(m-m_0)\phi_R} \chi_{i\ell SI m}^J(R, \theta_R). \end{aligned} \quad (9)$$

Coefficients $\sum_J \chi_{i\ell SI m}^J(R, \theta_R) \exp[-i(m-m_0)\phi_R]$ of the expansion show the c.m. motion of the projectile in the $\{i, \ell, S, I, m\}$ channel, where ℓ, S and I are the orbital angular momentum, the channel-spin and the total spin of ${}^8\text{B}$, respectively; the orbital angular momentum between ${}^8\text{B}$ and A is denoted by L , and J is the total angular momentum of the three-body system. The symbol m is the projection of I on the z -axis taken to be parallel to the incident beam, and m_0 is m in the initial state. For simplicity we below denote the five channel-indices $\{i, \ell, S, I, m\}$ as c .

We take the same Φ_c as CDCC [15, 16] does, which consist of bound-states and “discretized-continuum-states.” As for the prescription for calculating the latter, the average method [15, 16, 17, 37] and the pseudo-state methods [15, 38, 39, 40] are widely used. The Φ_c satisfy

$$\langle \Phi_{c'}(\mathbf{r}) | h | \Phi_c(\mathbf{r}) \rangle_{\mathbf{r}} = \epsilon_{i,\ell SI} \delta_{c'c}, \quad (10)$$

where h is the internal Hamiltonian defined by $h = T_r + V_{17}(\mathbf{r})$ and $\epsilon_{i,\ell SI}$ is the intrinsic energy corresponding to the channel $\{i, \ell, S, I\}$. As for the coupling scheme of angular momenta, we take the following form

$$\begin{aligned} \Phi_c(\mathbf{r}) &= \varphi_{i,\ell SI}(r) \sum_{m_\ell, m_S} (\ell m_\ell S m_S | I m) i^\ell Y_{\ell m_\ell}(\hat{\mathbf{r}}) \zeta_{S m_S} \\ &\equiv \varphi_{i,\ell SI}(r) [i^\ell Y_\ell(\hat{\mathbf{r}}) \otimes \zeta_S]_{I m}, \end{aligned} \quad (11)$$

where $Y_{\ell m_\ell}$ is the spherical harmonics and $\zeta_{S m_S}$ the spin wave function of the projectile with channel-spin S . It should be noted that $\Phi_0(\mathbf{r})$, where the subscript 0 represents the ground state of ${}^8\text{B}$, is nothing but $\psi_{17}(\mathbf{r})$ in Eq. (5). Since the Φ_c are chosen to form an approximate complete-set in a finite space being significant for a reaction concerned [38], the expansion of Eq. (9) is assumed to be accurate. Unknown coefficients $\chi_c^J(R, \theta_R)$ of the expansion are obtained by solving coupled-channel equations derived below.

Multiplying Eq. (8) by $\Phi_{c'}^*(\mathbf{r})$ from the left and integrating over \mathbf{r} and internal coordinates concerned with the spin lead to coupled equations for χ_c^J :

$$\begin{aligned} \sum_J e^{-im'\phi_R} (\mathcal{T}_R + \epsilon_{c'} - E_{\text{in}} - e_8) \chi_c^J(R, \theta_R) \\ = - \sum_c F_{c'c} \sum_J e^{-im\phi_R} \chi_c^J(R, \theta_R). \end{aligned} \quad (12)$$

The reduced kinetic-energy operator \mathcal{T}_R and the form factor $F_{c'c}$, in the cylindrical coordinate taken here, are defined by

$$\mathcal{T}_R = -\frac{\hbar^2}{2\mu}\nabla_R^2 + \frac{\hbar^2}{2\mu}\frac{(m' - m_0)^2}{b^2} \approx -\frac{\hbar^2}{2\mu}\nabla_R^2 = T_R, \quad (13)$$

$$\begin{aligned} F_{c'c}(\mathbf{R}) &= \langle \Phi_{c'} | V_{A7} + V_{A1} | \Phi_c \rangle_{\mathbf{r}} \\ &\equiv \mathcal{F}_{c'c}(R, \theta_R) e^{-i(m' - m)\phi_R}. \end{aligned} \quad (14)$$

In Eq. (13) μ is the reduced mass of the ^8B -A system and the impact parameter b is given by $b = \sqrt{x^2 + y^2}$ for the vector $\mathbf{R} = (x, y, z)$; we have neglected the weak-dependence of \mathcal{T}_R on b , which turned out to have no effect on numerical results in the present case. In Eq. (14) we assume V_{A7} and V_{A1} to be central interactions; this assumption is valid, as discussed in Ref. [31], since we use E-CDCC only to obtain the scattering amplitude for large values of b . The explicit form of the coupling potentials $\mathcal{F}_{c'c}$ is then

$$\begin{aligned} \mathcal{F}_{c'c}(R, \theta_R) &= \sum_{\lambda} i^{\ell - \ell'} \sqrt{4\pi} (-)^{2I' + m - S} \\ &\times \sqrt{\frac{(2\ell + 1)(2\ell' + 1)(2I + 1)(2I' + 1)}{(2\lambda + 1)^3}} \\ &\times (I - m I' m' | \lambda m' - m)(\ell 0 \ell' 0 | \lambda 0) \\ &\times W(\ell \ell' I I'; \lambda S) \delta_{S' S} \\ &\times C_{\lambda m' - m} P_{\lambda m' - m}(\cos \theta_R) \\ &\times \int \varphi_{i', \ell' S' I'}^*(r) \mathcal{U}^{(\lambda)}(R, r) \varphi_{i, \ell S I}(r) r^2 dr, \end{aligned}$$

where $W(\ell \ell' I I'; \lambda S)$ is the Racah coefficient and

$$C_{\lambda\nu} \equiv (-)^{(\nu + |\nu|)/2} \sqrt{\frac{2\lambda + 1}{4\pi} \frac{(\lambda - |\nu|)!}{(\lambda + |\nu|)!}}.$$

The λ th-order multipole $\mathcal{U}^{(\lambda)}$ is defined by $\mathcal{U}^{(\lambda)}(R, r) = u_{A7}^{(\lambda)}(R, r/8) + u_{A1}^{(\lambda)}(R, 7r/8)$ with

$$\begin{aligned} U_{A7}(R_{A7}) &= \sum_{\lambda} u_{A7}^{(\lambda)}(R, r/8) \frac{4\pi}{\lambda^2} \sum_{\nu} Y_{\lambda\nu}^*(\hat{\mathbf{R}}) Y_{\lambda\nu}(\hat{\mathbf{r}}), \\ U_{A1}(R_{A1}) &= \sum_{\lambda} u_{A1}^{(\lambda)}(R, 7r/8) \frac{4\pi}{\lambda^2} \sum_{\nu} Y_{\lambda\nu}^*(\hat{\mathbf{R}}) Y_{\lambda\nu}(\hat{\mathbf{r}}). \end{aligned}$$

Now we make the Coulomb-eikonal approximation [41] to χ_c^J :

$$\chi_c^J(R, \theta_R) \approx \xi_c^J(b, z) \phi_c^{C(+)}(b, z). \quad (15)$$

In Eq. (15) $\phi_c^{C(+)}$ is the outgoing Coulomb-wave-function:

$$\begin{aligned} \phi_c^{C(+)}(b, z) &= \frac{e^{-\pi\eta_c/2}}{(2\pi)^{3/2}} \Gamma(1 + i\eta_c) e^{i\mathbf{K}_c \cdot \mathbf{R}} F_{\mathbf{K}_c}^c(\mathbf{R}), \\ F_{\mathbf{K}_c}^c(\mathbf{R}) &\equiv G(-i\eta_c, 1, i(K_c R - \mathbf{K}_c \cdot \mathbf{R})) \end{aligned}$$

with Γ the Gamma function and G the confluent hypergeometric function. In actual calculation we make use of the approximate asymptotic-form of $\phi_c^{C(+)}$,

$$\begin{aligned} \phi_c^{C(+)}(b, z) &\sim \frac{1}{(2\pi)^{3/2}} \left(1 + \frac{\eta_c^2}{i(K_c R - \mathbf{K}_c \cdot \mathbf{R})} + \dots \right) \\ &\times e^{i(\mathbf{K}_c \cdot \mathbf{R} + \eta_c \ln(K_c R - \mathbf{K}_c \cdot \mathbf{R}))} \\ &\approx \frac{1}{(2\pi)^{3/2}} e^{i(K_c z + \eta_c \ln(K_c R - K_c z))}, \end{aligned} \quad (16)$$

which is valid for large values of b . The boundary condition for ξ_c^J in Eq. (15) is $\lim_{z \rightarrow -\infty} \xi_c^J(b, z) = \delta_{c0}$, where 0 denotes the incident channel. Then, the scattering wave-function χ_c^J satisfies the appropriate boundary condition at $z \rightarrow -\infty$.

We here make the following two approximations, just in the same way as in Ref. [31]. (i) For sufficiently large b , the flux of $\phi_c^{C(+)}$ is assumed to be parallel to the z -axis. (ii) We make the local semiclassical approximation [42] to $\phi_c^{C(+)}$,

$$\frac{\partial \phi_c^{C(+)}(b, z)}{\partial z} \approx iK_c(R) \phi_c^{C(+)}(R), \quad (17)$$

which is valid for a wave function under a slowly-varying potential. The local wave number $K_c(R)$ is defined by

$$\frac{\hbar^2}{2\mu} K_c^2(R) = E_{\text{in}} + e_8 - \epsilon_c - \frac{Z_8 Z_A e^2}{R}, \quad (18)$$

where $Z_8 e$ ($Z_A e$) represents the charge of ^8B (A). Further approximation to $\phi_c^{C(+)}$ was made in Ref. [31], i.e. the c -dependence of $F_{\mathbf{K}_c}^c$ was neglected. On the contrary, in the present paper we solve coupled-channel equations taking account of that dependence by using Eq. (16). This treatment of the Coulomb wave function turned out to slightly improve the agreement between the quantum-mechanical and eikonal scattering-amplitudes for large L .

In consequence of Eq. (13) and the Coulomb-eikonal approximation, one finds

$$\begin{aligned} \mathcal{T}_R \chi_c^J(R, \theta_R) &\approx T_R \left(\xi_c^J(b, z) \phi_c^{C(+)}(b, z) \right) \\ &\approx \left[-\frac{i\hbar^2}{\mu} K_c(R) \left(\frac{\partial \xi_c^J(b, z)}{\partial z} \right) \right. \\ &\quad \left. + \left(T_R \phi_c^{C(+)}(b, z) \right) \xi_c^J(b, z) \right] \phi_c^{C(+)}(b, z), \end{aligned} \quad (19)$$

where the second-order derivative of ξ_c^J has been neglected since it is slowly varying compared with the remainder $\phi_c^{C(+)}(b, z)$. Inserting Eqs. (14), (16), (19) and

$$T_R \phi_c^{C(+)}(b, z) = \left(E_{\text{in}} + e_8 - \epsilon_c - \frac{Z_8 Z_A e^2}{R} \right) \phi_c^{C(+)}(b, z) \quad (20)$$

into Eq. (12), one reaches to the following coupled-channel equations

$$\frac{i\hbar^2}{\mu}K_c(R)\frac{d}{dz}\psi_c^{(b)}(z) = \sum_{c'}\mathfrak{F}_{cc'}^{(b)}(z)\mathcal{R}_{cc'}^{(b)}(z)\psi_{c'}^{(b)}(z) \times e^{i(K_{c'}-K_c)z}, \quad (21)$$

where $\psi_c^{(b)}(z) \equiv \sum_J \xi_c^J(b, z)$; we have put the non-dynamical variable b in a superscript and commuted c and c' . The reduced coupling-potential $\mathfrak{F}_{cc'}$ is defined by

$$\mathfrak{F}_{cc'}^{(b)}(z) = \mathcal{F}_{cc'}^{(b)}(z) - \frac{Z_8 Z_A e^2}{R} \delta_{cc'} \quad (22)$$

and

$$\mathcal{R}_{cc'}^{(b)}(z) \equiv \frac{e^{i\eta_{c'} \ln(K_{c'}R - K_{c'}z)}}{e^{i\eta_c \ln(K_cR - K_cz)}} = \frac{(K_{c'}R - K_{c'}z)^{i\eta_{c'}}}{(K_cR - K_cz)^{i\eta_c}}. \quad (23)$$

Since the E-CDCC equation has the first-order differential form and contains no coefficient with huge angular-momentum, one can solve it with high computational speed and accuracy.

The eikonal scattering amplitude with Coulomb distortion is given by $f_{c0}^E = f_{c0}^{\text{Ruth}}\delta_{c0} + f_{c0}'^E$, where f_{c0}^{Ruth} is the Rutherford amplitude and

$$f_{c0}'^E \equiv -\frac{(2\pi)^2\mu}{\hbar^2} \int \sum_{c'} \mathfrak{F}_{cc'}^{(b)}(z) \phi_c^{*C(-)}(b, z) \phi_{c'}^{C(+)}(b, z) \times e^{-i(m-m_0)\phi_R} \psi_{c'}^{(b)}(z) d\mathbf{R} \quad (24)$$

with

$$\begin{aligned} \phi_c^{C(-)}(b, z) &= \frac{e^{-\pi\eta_c/2}}{(2\pi)^{3/2}} \Gamma^*(1 + i\eta_c) e^{i\mathbf{K}'_c \cdot \mathbf{R}} F_{-\mathbf{K}'_c}^{C*}(\mathbf{R}) \\ &\approx \frac{1}{(2\pi)^{3/2}} e^{i\mathbf{K}'_c \cdot \mathbf{R}} e^{-i\eta_c \ln(K_cR + \mathbf{K}'_c \cdot \mathbf{R})}. \end{aligned} \quad (25)$$

The outgoing c.m. momentum $\hbar\mathbf{K}'_c$ is chosen to be on the z - x plane, following the Madison convention. We here assume forward scattering just in the same way as in Ref. [31], i.e. the phase-factor $(\mathbf{K}_{c'} - \mathbf{K}_c) \cdot \mathbf{R}$, which appears in $\phi_c^{*C(-)}(b, z) \phi_{c'}^{C(+)}(b, z)$, is approximated by $-K_c\theta_f b \cos\phi_R + (K_{c'} - K_c)z$, where θ_f is the scattering angle of ${}^8\text{B}$. Furthermore, we replace $K_cR + \mathbf{K}'_c \cdot \mathbf{R}$ in Eq. (25) by $K_cR + K_cz$. One then finds

$$\begin{aligned} f_{c0}'^E &= -\frac{\mu}{2\pi\hbar^2} \int e^{-i(m-m_0)\phi_R} e^{-iK_c \sin\theta_f b \cos\phi_R} bdbd\phi_R \\ &\quad \times \mathcal{H}_c^{(b)} \int \sum_{c'} \mathfrak{F}_{cc'}^{(b)}(z) \psi_{c'}^{(b)}(z) e^{i(K_{c'}-K_c)z} \mathcal{R}_{cc'}^{(b)}(z) dz, \end{aligned} \quad (26)$$

with $\mathcal{H}_c^{(b)} \equiv \exp[2i\eta_c \ln(K_c b)]$.

The integration over z in Eq. (26) can be done analytically with the help of Eq. (21), i.e.

$$\begin{aligned} \mathcal{I} &\equiv \int \sum_{c'} \mathfrak{F}_{cc'}^{(b)}(z) \psi_{c'}^{(b)}(z) e^{i(K_{c'}-K_c)z} \mathcal{R}_{cc'}^{(b)}(z) dz \\ &= \frac{i\hbar^2}{\mu} \int K_c(R) \left(\frac{d}{dz} \psi_c^{(b)}(z) \right) dz \\ &\approx \frac{i\hbar^2}{\mu} \left[K_c(R) \psi_c^{(b)}(z) \right]_{-\infty}^{\infty} \\ &\equiv \frac{i\hbar^2}{\mu} K_c \left[\mathcal{S}_{c0}^{(b)} - \delta_{c0} \right], \end{aligned} \quad (27)$$

where we have neglected $\partial K_c(R)/\partial z$, since $K_c(R)$, with large b , is a slowly-varying function of z . The eikonal S -matrix elements are defined by $\mathcal{S}_{c0}^{(b)} = \lim_{z \rightarrow \infty} \psi_c^{(b)}(z)$. Inserting Eq. (27) into Eq. (26) leads to

$$\begin{aligned} f_{c0}'^E &\approx \frac{K_c}{2\pi i} \int e^{-i(m-m_0)\phi_R} e^{-iK_c \sin\theta_f b \cos\phi_R} bdbd\phi_R \\ &\quad \times \mathcal{H}_c^{(b)} \left[\mathcal{S}_{c0}^{(b)} - \delta_{c0} \right]. \end{aligned} \quad (28)$$

We here transform the integration over b to the summation over L , just in the same way as in Ref. [31]. The resulting eikonal amplitude is

$$\begin{aligned} f_{c0}'^E &= \frac{2\pi}{iK_0} \sum_L \frac{K_0}{K_c} \mathcal{H}_c^{(b_{c;L})} \sqrt{\frac{2L+1}{4\pi}} i^{(m-m_0)} \\ &\quad \times \left[\mathcal{S}_{c0}^{(b_{c;L})} - \delta_{c0} \right] Y_{Lm-m_0}(\hat{\mathbf{K}}') \\ &\equiv \frac{2\pi}{iK_0} \sum_L f_{L;c0}'^E Y_{Lm-m_0}(\hat{\mathbf{K}}') \end{aligned} \quad (29)$$

with $K_c b_{c;L} = L + 1/2$. The quantum-mechanical scattering amplitude, which is obtained by CDCC, is given by

$$\begin{aligned} f_{c0}'^Q &= \frac{2\pi}{iK_0} \sum_L \sum_{J=|L-I|}^{L+I} \sum_{L_0=|J-I_0|}^{J+I_0} \sqrt{\frac{2L_0+1}{4\pi}} \\ &\quad \times (I_0 m_0 L_0 | J m_0) (I m L m_0 - m | J m_0) \\ &\quad \times (S_{iLlSI, i_0 L_0 \ell_0 S_0 I_0}^J - \delta_{i_0} \delta_{L L_0} \delta_{\ell \ell_0} \delta_{S S_0} \delta_{I I_0}) \\ &\quad \times e^{i(\sigma_L + \sigma_{L_0})} (-)^{m-m_0} Y_{Lm-m_0}(\hat{\mathbf{K}}') \\ &\equiv \frac{2\pi}{iK_0} \sum_L f_{L;c0}'^Q Y_{Lm-m_0}(\hat{\mathbf{K}}'), \end{aligned} \quad (30)$$

where σ_L is the Coulomb phase shift. The hybrid scattering amplitude is defined by

$$\begin{aligned} f_{c0}^H &= f_{c0}^{\text{Ruth}} \delta_{c0} + \frac{2\pi}{iK_0} \sum_{L < L_C} f_{L;c0}'^Q Y_{Lm-m_0}(\hat{\mathbf{K}}') \\ &\quad + \frac{2\pi}{iK_0} \sum_{L \geq L_C} f_{L;c0}'^E Y_{Lm-m_0}(\hat{\mathbf{K}}'), \end{aligned} \quad (31)$$

which is used in the present analysis of ${}^8\text{B}$ breakup. The connecting-angular-momentum L_C between quantum-mechanical and eikonal amplitudes is chosen so that $f_{L;c0}'^E$

agrees with $f_{L;c0}^Q$ for $L \geq L_C$. It should be noted that Eq. (31) includes all quantum effects and also the interference between amplitudes in the two L -regions. This hybrid CDCC calculation turned out to describe nuclear and Coulomb breakup with very high accuracy and computational speed. Actually, it was found that the accuracy is the same as that of fully quantum-mechanical CDCC and the computation time is almost as 1/10 as that of standard CDCC calculation.

III. RESULTS AND DISCUSSION

A. Numerical calculation

As for the wave function of ${}^8\text{B}$, we adopt a single-particle model. The ground state of ${}^8\text{B}$ then contains the following three components: (a) ${}^7\text{Be}(3/2^-) \otimes p(1/2^-)$, (b) ${}^7\text{Be}(3/2^-) \otimes p(3/2^-)$ and (c) ${}^7\text{Be}(1/2^-) \otimes p(3/2^-)$. In configuration (c), the binding energy of p in ${}^8\text{B}$ is large, because of the excitation energy of ${}^7\text{Be}$. The corresponding single-particle wave function $\psi_{17}(\mathbf{r})$ thus falls-off rapidly as r increases, compared with those corresponding to (a) and (b). Thus, the component (c) has no contribution to $S_{17}(E)$, since the ${}^7\text{Be}(p, \gamma){}^8\text{B}$ reaction is described only by the wave function in the tail region at stellar energies. It should be noted that the excited-core component (c) is not included in the experimental data measured at RIKEN, GSI and MSU [7, 8, 9, 10, 11, 12, 13]. In asymptotic region $r > R_N$, $\mathfrak{S}_{\text{exp}}\psi_{17}(\mathbf{r})$ is then written by

$$\begin{aligned} \mathfrak{S}_{\text{exp}}\psi_{17}(\mathbf{r}) = & \left\{ C_{\frac{1}{2}} \left[\left[iY_1(\hat{\mathbf{r}}) \otimes \varsigma_{\frac{1}{2}} \right]_{\frac{1}{2}} \otimes \varsigma_{\frac{3}{2}} \right]_{2m_0} \right. \\ & \left. + C_{\frac{3}{2}} \left[\left[iY_1(\hat{\mathbf{r}}) \otimes \varsigma_{\frac{1}{2}} \right]_{\frac{3}{2}} \otimes \varsigma_{\frac{3}{2}} \right]_{2m_0} \right\} \\ & \times \frac{W_{-\eta, 3/2}(2k_0 r)}{r}, \quad r > R_N, \end{aligned} \quad (32)$$

where $\varsigma_{1/2}$ ($\varsigma_{3/2}$) is the spin- $\frac{1}{2}$ (spin- $\frac{3}{2}$) wave function. The ratio of the ANC for configuration (a) to that for (b) was determined by microscopic calculation [29], i.e. $C_{1/2}^2/C_{3/2}^2 = 0.157$.

In actual calculation, as already mentioned, we take a normalized single particle wave function $f_0(r)$ for the radial part of $\psi_{17}(\mathbf{r})$, which in principle depends on the configuration of ${}^8\text{B}$. In the ANC approach, however, $S_{17}(0)$ is determined from the comparison between theoretical and experimental results at forward angles, where the inner part of the ${}^8\text{B}$ wave function has no contribution. Therefore, one can use

$$\begin{aligned} \psi_{17}(\mathbf{r}) = & \left\{ P' \left[iY_1(\hat{\mathbf{r}}) \otimes \left[\varsigma_{\frac{1}{2}} \otimes \varsigma_{\frac{3}{2}} \right]_{S=1} \right]_{2m_0} \right. \\ & \left. + Q' \left[iY_1(\hat{\mathbf{r}}) \otimes \left[\varsigma_{\frac{1}{2}} \otimes \varsigma_{\frac{3}{2}} \right]_{S=2} \right]_{2m_0} \right\} f_0(r), \end{aligned} \quad (33)$$

where

$$\begin{aligned} P' &= -\sqrt{6} W(1 \ 2 \ 1/2 \ 1/2; 1 \ 3/2) P \\ &\quad + 2\sqrt{3} W(1 \ 2 \ 1/2 \ 3/2; 1 \ 3/2) Q \sim 0.397, \\ Q' &= \sqrt{10} W(2 \ 2 \ 1/2 \ 1/2; 1 \ 3/2) P \\ &\quad - 2\sqrt{5} W(2 \ 2 \ 1/2 \ 3/2; 1 \ 3/2) Q \sim 0.918 \end{aligned}$$

with $P^2 = C_{1/2}^2/(C_{1/2}^2 + C_{3/2}^2)$ and $Q^2 = C_{3/2}^2/(C_{1/2}^2 + C_{3/2}^2)$. In Eq. (33) we have changed the coupling scheme of angular-momenta from the spin-orbit representation to the channel-spin one.

Since we concentrate on forward scattering of ${}^8\text{B}$, spin-dependent interactions between the target nucleus and each constituent of ${}^8\text{B}$ can be neglected. The channel-spin S is then fixed during the breakup process of ${}^8\text{B}$ [15]. Thus, one can separately treat the $S = 1$ and $S = 2$ components in Eq. (33) and calculate breakup cross sections corresponding to them: $\sigma_{S=1}$ and $\sigma_{S=2}$. Furthermore, for given values of S and ℓ , the p - ${}^7\text{Be}$ interaction is independent of I . This is because the excitation energy of ${}^8\text{B}$ concerned is quite small compared with the centrifugal barrier between p and ${}^7\text{Be}$; it should be noted that for $\ell = 0$ there is no splitting of I . Consequently, the internal wave functions of ${}^8\text{B}$ with fixed S and ℓ and different values of I degenerate, which greatly simplifies numerical calculation. Thus, with the help of Eq. (33) one can calculate the cross section σ that takes account of the intrinsic spin of ${}^8\text{B}$: $\sigma = P'^2 \sigma_{S=1} + Q'^2 \sigma_{S=2}$. The value of \bar{a}_s in Eq. (2) corresponding to the spin-dependent ANC analysis is [32] $\bar{a}_s = P'^2 a_s^{S=1} + Q'^2 a_s^{S=2}$ fm, where $a_s^{S=1}$ and $a_s^{S=2}$ are the p - ${}^7\text{Be}$ scattering length for the $S = 1$ and $S = 2$ channels, respectively.

For the p -state of ${}^8\text{B}$ in both $S = 1$ and $S = 2$ channels, the single-particle potential of Esbensen and Bertsch (EB) [43] is used. Since we adopt the channel-spin representation, we neglect the spin-orbit part of the potential and adjust the depth of the central potential to reproduce the separation energy of p , 137 keV. For d - and f -states with both $S = 1$ and $S = 2$, we use the potential of Barker [44]. We found by numerical calculation that the results shown below are independent of the single-particle potentials for the d - and f -states. For the s -state in the $S = 2$ channel, we use the potential of Barker that gives the scattering length $a_s^{S=2}$ of -8 fm. This value is consistent with the experimental result, i.e. -7 ± 3 fm [45]. For the s -state with $S = 1$, we change the depth of the potential of Barker to 25.7 MeV so that the resulting scattering length is 25 fm; the experimental value is $a_s^{S=1} = 25 \pm 9$ fm.

As for the distorting potential between p (${}^7\text{Be}$) and ${}^{208}\text{Pb}$ we adopt the global optical potential by Koning and Delaroche [46] (Cook [47]). We neglect the spin-orbit parts of the p - ${}^{208}\text{Pb}$ potential as mentioned above. The multipoles for nuclear and Coulomb coupling-potentials are included up to $\lambda = 6$. The discretized-continuum states of ${}^8\text{B}$ are constructed by the average method [15, 16, 17, 37]. The maximum excitation energy of ${}^8\text{B}$ is 10 MeV and 10, 20, 10 and 5 discretized-continuum states are taken for $\ell = 1, 0, 2$ and 3 states, respectively. The resulting number of scattering-channels in CDCC is 138. The maximum values of r , R and L are, respectively,

200 fm, 1000 fm and 12000. The above modelspace turned out to give good convergence of the resulting breakup-cross-sections.

B. Analysis of ${}^8\text{B}$ breakup experiment

Figure 3 shows the convergence of the hybrid calculation with CDCC and E-CDCC for ${}^{208}\text{Pb}({}^8\text{B}, p+{}^7\text{Be}){}^{208}\text{Pb}$ at 52 MeV/nucleon. The breakup cross section of ${}^8\text{B}$ integrated over the excitation energy of ${}^8\text{B}$, ε_8 , from 500 keV to 750 keV is plotted as a function of θ_8 . The dashed line is the result of the E-CDCC calculation ($L_C = 0$) and the dotted, dash-dotted and solid lines correspond to the hybrid calculation with $L_C = 500, 1000$ and 1500 , respectively. The figure shows that the hybrid calculation converges with $L_C = 1000$. The difference between the dash-dotted and solid lines is only less than about 1% in magnitude. Thus, below we regard the hybrid calculation of CDCC and E-CDCC with $L_C = 1000$ as the fully quantum-mechanical CDCC calculation.

One sees in Fig. 3 the oscillation of the cross section at forward angles around 2° , which turned out to be due to the interference between nuclear and Coulomb breakup-amplitudes. Therefore, it can be concluded that nuclear interactions affect the breakup cross section even at very forward angles. However, as one sees below, this oscillation is not observed in actual experimental data because of the limit of the resolution of θ_8 for the measurement.

Figure 4 shows the comparison between CDCC calculation and the experimental data for the ${}^8\text{B}$ breakup. In order to take account of the experimental resolution and efficiency, the theoretical result has been smeared out by using the filtering-table [48] provided by the authors of Ref. [8]. The upper panel shows the filtering effect on the calculated cross sec-

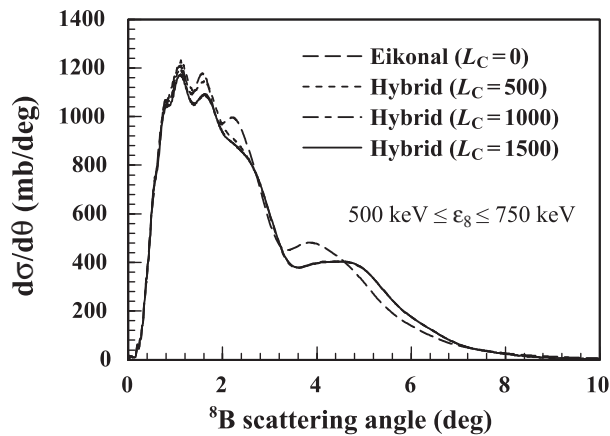


FIG. 3: The ${}^8\text{B}$ breakup cross section as a function of the scattering angle of the c.m. of ${}^8\text{B}$. The cross section has been integrated over the excitation energy of ${}^8\text{B}$, ε_8 , measured from the $p+{}^7\text{Be}$ threshold energy, in the range of 500–750 keV. The dotted, dash-dotted and solid lines represent the results of the hybrid calculation of CDCC and E-CDCC with $L_C = 500, 1000$ and 1500 , respectively. The result of E-CDCC, i.e. $L_C = 0$, is also shown by the dashed line.

tion, where the solid and dashed lines represent the results of CDCC obtained with and without the smearing procedure. In the lower panel, the total breakup cross section calculated with CDCC is decomposed into the s- (dashed line), p- (dotted line), d- (dash-dotted line) and f-state (dash-two-dotted line) breakup components of ${}^8\text{B}$.

One sees the smeared result of CDCC well agrees with the experimental data at forward angles ($\theta_8 \lesssim 4^\circ$), while it underestimates the data at backward angles. The lower panel shows the importance of the p-state breakup for $\theta_8 \gtrsim 5^\circ$, which implies that nuclear breakup is significant in this angular region. Thus, careful description of ${}^8\text{B}$ wave function, the resonance structures of it in particular, will be necessary to reproduce the experimental data at backward angles. Moreover, as discussed in Sec. II B, the excited-core component in ${}^8\text{B}$, ${}^7\text{Be}(1/2^-) \otimes p(3/2^-)$, may dynamically play an important role there. Although further study in this line will be very interesting, it is beyond the scope of the present paper. Additionally, the filtering-table used was made with assuming the s-state breakup of ${}^8\text{B}$. Thus, quantitative comparison between

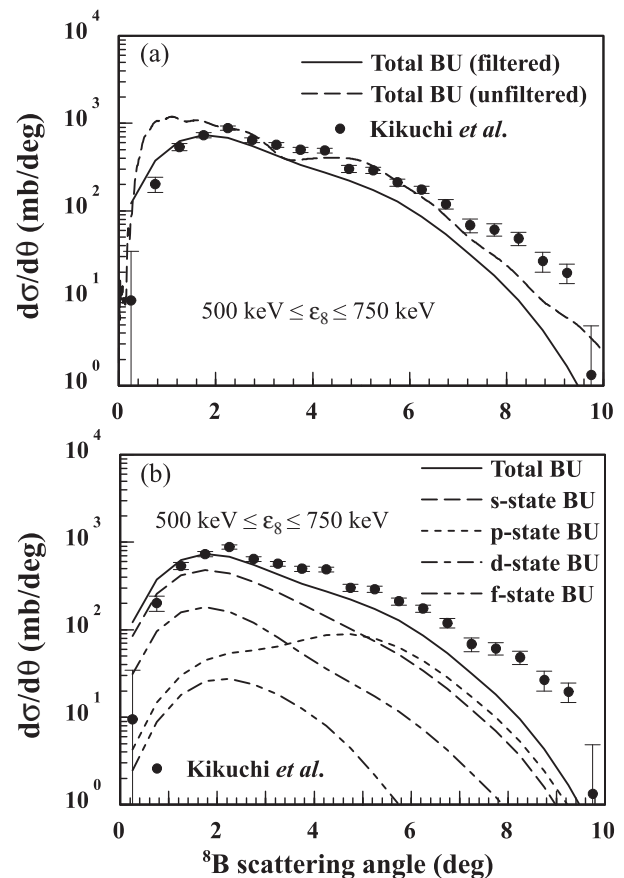


FIG. 4: (a) The calculated ${}^8\text{B}$ breakup cross sections with (solid line) and without (dashed line) taking account of the resolution and efficiency of the measurement [48]. The experimental data are taken from Ref. [8]. (b) Decomposition of the ${}^8\text{B}$ breakup cross section into the s- (dashed line), p- (dotted line), d- (dash-dotted line) and f-state (dash-two-dotted line) breakup components.

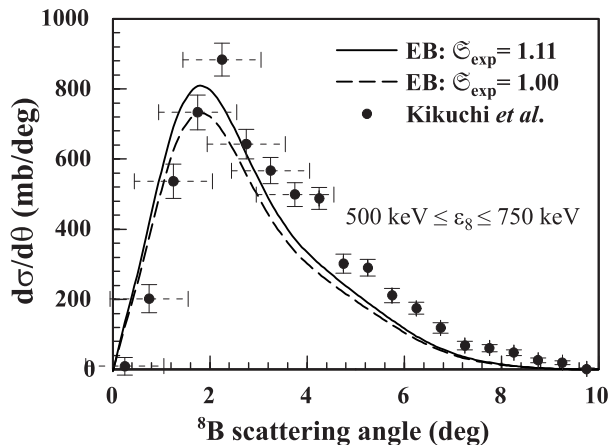


FIG. 5: The result of the χ^2 -fit of the breakup cross section calculated with the ^8B single-particle potential of Esbensen and Bertsch (EB) [43]. The solid line is the same as that in the top panel in Fig. 4 but multiplied by the spectroscopic factor $\Xi_{\text{exp}} = 1.11$. The result with $\Xi_{\text{exp}} = 1.00$ is also shown by the dashed line for comparison. For the eight data points below 4° , which are used in the fitting procedure, we have put the horizontal bar that represents the resolution of θ_8 [8] for the measurement.

the calculation and the experimental data, to extract $S_{17}(0)$ with high accuracy, can only be done in the region where the s-state breakup cross section is dominant. Therefore, below we use the data for $\theta_8 \leq 4^\circ$ to determine Ξ_{exp} by Eq. (3).

Figure 5 shows the result of the χ^2 -fit of the theoretical calculation to the experimental data. The solid line is the same as that in the upper panel in Fig. 4 but multiplied by the spectroscopic factor $\Xi_{\text{exp}} = 1.11$. The dashed line represents the result before being fitted, i.e. with $\Xi_{\text{exp}} = 1.00$. Each horizontal bar put on the eight data points below 4° does not represent a statistical error but it shows the range of θ_8 in which the breakup cross sections contribute to each data point [8]. The value of χ^2 per datum obtained is 8.5. Although the quality of the fit is not good, it should be noted that estimation of error-propagation in the present case, i.e. comparison between smeared experimental data and a smeared numerical result, is very complicated; the value of χ^2 per datum shown above takes account of no error with respect to θ_8 . The single-particle ANC corresponding to the EB ^8B wavefunction is $\alpha = 0.704 \text{ fm}^{-1/2}$. With the values of Ξ_{exp} and α , the ANC C is obtained from Eq. (3) as $C = 0.740 \text{ fm}^{-1/2}$. One can then determine $S_{17}(0)$ by inserting this result into Eq. (2), together with the value of the averaged scattering-length $\bar{a}_s = -2.8 \text{ fm}$, i.e. $S_{17}(0) = 20.9 \text{ eV b}$. In the next subsection we quantitatively evaluate uncertainties of the extracted $S_{17}(0)$.

C. Uncertainties of the extracted $S_{17}(0)$

First, we evaluate the uncertainty of $S_{17}(0)$ that comes from the use of the ANC method, just in the same way as in

Refs. [25, 28]. We show in Fig. 6 the result of CDCC calculation with the p-state single-particle potential of ^8B by Kim *et al.* [49] (the dashed line) and that multiplied by $\Xi_{\text{exp}} = 0.867$ (the solid line); the latter agrees with the result shown in Fig. 5 within 1% in error. One sees that Ξ_{exp} indeed depends on the p-state potential. Actually, the single-particle ANC for Kim's

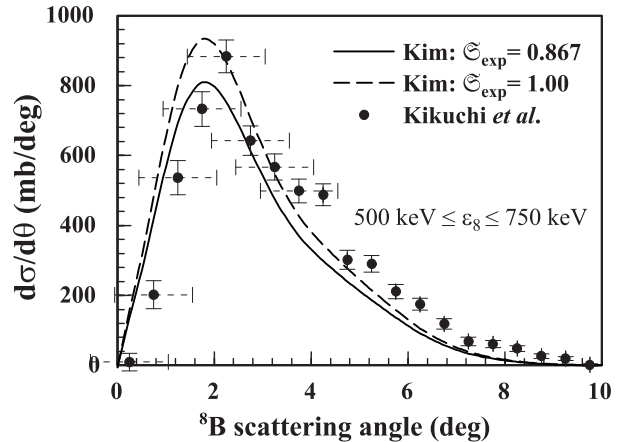


FIG. 6: Same as in Fig. 5 but for the CDCC calculation with Kim's single-particle potential [49] for the p-state of ^8B ; the spectroscopic factor obtained is 0.867. The result with Kim's potential before χ^2 -fitting, namely with $\Xi_{\text{exp}} = 1.00$, is also shown by the dashed line for comparison.

potential is $0.796 \text{ fm}^{-1/2}$, which quite differs from the value for the EB potential, $0.704 \text{ fm}^{-1/2}$, because of the difference in the geometry of the two potentials of about 20%. On the contrary, the resulting value of ANC with Kim's potential is $0.741 \text{ fm}^{-1/2}$ that very well agrees with the result obtained with the EB potential. This result shows that the ANC method works with very high accuracy in the present analysis, i.e. the error of the ANC method is negligibly small.

Second, we estimate effects of ambiguity of the distorting potentials used in the CDCC calculation on $S_{17}(0)$. For this purpose we prepare alternative optical potentials for p - ^{208}Pb and ^7Be - ^{208}Pb . For the former, we modify the parameter set of Koning and Delaroche so that the calculated elastic cross section without spin-orbit terms reproduces the result with the full components of the optical potential. The parameter set thus obtained is $V_V = 39.82 \text{ MeV}$, $W_V = 0.776 \text{ MeV}$ and $W_D = 13.47 \text{ MeV}$, with the same notation as in Ref. [46]; all other parameters are not changed. For the latter, we use a single-folding model with the nucleon- ^{208}Pb potential of Koning and Delaroche. The density distribution of ^7Be is assumed to be the Gaussian form and the range of the Gaussian is determined to reproduce the rms matter radius of ^7Be , 2.48 fm [50]. The difference between the results calculated with the original and alternative optical potentials was found to be negligibly small (not shown). Therefore, we conclude that the error of $S_{17}(0)$ that comes from the ambiguity of the distorting potentials is negligibly small in the present case.

Finally, we discuss the ambiguity of the s-state single-particle potentials of ^8B for the $S = 1$ and $S = 2$ channels.

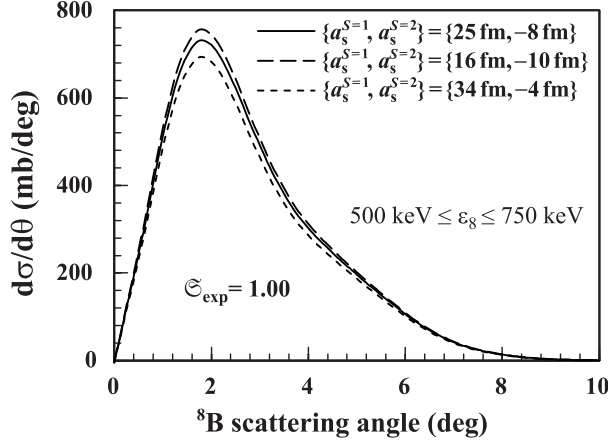


FIG. 7: Dependence of the ${}^8\text{B}$ breakup cross section on the single-particle potential for the s-state of ${}^8\text{B}$. The solid line represents the result with the choice of the single-particle potentials that corresponds to the scattering length $\{a_s^{S=1}, a_s^{S=2}\} = \{25 \text{ fm}, -8 \text{ fm}\}$. The dashed (dotted) line shows the result with the s-state potentials corresponding to $\{a_s^{S=1}, a_s^{S=2}\} = \{16 \text{ fm}, -10 \text{ fm}\}$ ($\{34 \text{ fm}, -4 \text{ fm}\}$).

We estimate the uncertainty of $S_{17}(0)$ concerned with this ambiguity by changing the depth of the s-state potential for the $S = 1$ ($S = 2$) channel ranging from 23.3 MeV (52.80 MeV) to 30.5 MeV (57.55 MeV), which corresponds to the range of the resulting scattering-length $a_s^{S=1}$ ($a_s^{S=2}$) from 16 fm (−10 fm) to 34 fm (−4 fm), i.e. the range of the experimental values of a_s [45]. In Fig. 7 the solid, dashed and dotted lines represent the results with the s-state potentials corresponding to $\{a_s^{S=1}, a_s^{S=2}\} = \{25 \text{ fm}, -8 \text{ fm}\}$, $\{16 \text{ fm}, -10 \text{ fm}\}$ and $\{34 \text{ fm}, -4 \text{ fm}\}$, respectively. One sees the breakup cross section slightly depends on the choice of the s-state potentials of ${}^8\text{B}$; the resulting $S_{17}(0)$ is found to vary from 20.3 eV b to 21.9 eV b. Thus, we evaluate the error of $S_{17}(0)$ to be +4.9%/−2.9%.

The main result of $S_{17}(0)$ in the present paper is derived as follows. The central value of $S_{17}(0)$ is 20.9 eV b. The theoretical error of the extracted $S_{17}(0)$ concerned with the p - ${}^7\text{Be}$ scattering length is +4.9%/−2.9%. After including the 8.4% systematic experimental error, we obtain

$$S_{17}(0) = 20.9_{-0.6}^{+1.0} \text{ (theo)} \pm 1.8 \text{ (expt)} \text{ eVb.}$$

D. Discussion of the extracted $S_{17}(0)$

The main result of $S_{17}(0)$ in the present paper derived from ${}^{208}\text{Pb}({}^8\text{B}, p+{}^7\text{Be}){}^{208}\text{Pb}$ at 52 MeV/nucleon is $S_{17}(0) = 20.9_{-0.6}^{+1.0} \text{ (theo)} \pm 1.8 \text{ (expt)} \text{ eV b}$. This value is consistent with the result of the precise direct measurement [4], $S_{17}(0) = 22.1 \pm 0.6 \text{ (expt)} \pm 0.6 \text{ (theo)} \text{ eV b}$, and significantly larger than that obtained in the previous analysis of the same experiment with the first-order perturbation theory, $S_{17}(0) = 18.9 \pm 1.8 \text{ eV b}$ [9]. In order to clarify the reason for the difference, we here discuss roles of nuclear interaction, E2 transitions and higher-order processes. In Fig. 8 the

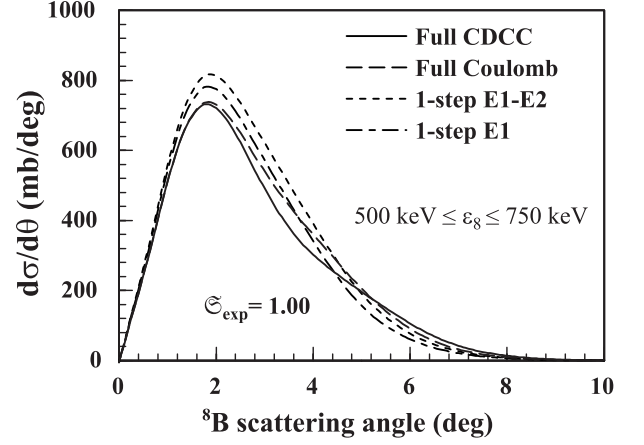


FIG. 8: The dashed line represents the result of full CDCC without nuclear breakup. The dash-dotted line is the result of one-step CDCC including only the Coulomb E1 coupling potentials, that corresponds to the first-order perturbation theory. The dotted-line shows the result of one-step CDCC with Coulomb E1 and E2 components. The result of CDCC with nuclear and Coulomb couplings and all higher-order processes is also shown by the solid line for comparison.

solid line shows the result of full CDCC that is the same as in the upper panel in Fig. 4. The dashed line corresponds to the calculation without breakup-components of nuclear coupling-potentials. It should be noted that the diagonal-components of them are included in the calculation to take account of the absorption of the incident flux by the target nucleus. One sees that the dashed line agrees with the solid line below 2° but deviate from it for $\theta_8 > 2^\circ$. As a result, the value of $S_{17}(0)$ calculated with neglecting nuclear breakup is smaller than that obtained with full CDCC calculation, i.e. $S_{17}(0) = 20.0_{-1.8}^{+1.9} \text{ eV b}$ is obtained.

The dash-dotted line in Fig. 8 represents the result of one-step CDCC without nuclear breakup-components, including only $\lambda = 1$ (E1) component; this calculation can be assumed to essentially correspond to the first-order perturbation theory (virtual photon theory) used in the previous analysis of the experimental data [9]. The dash-dotted line slightly overestimates the solid line above 1.5° and the resulting value of $S_{17}(0)$ is $19.0_{-1.7}^{+1.9} \text{ eV b}$, which well agrees with the value obtained in Ref. [9], $18.9 \pm 1.8 \text{ eV b}$.

If one includes the $\lambda = 2$ (E2) component in the Coulomb one-step calculation with CDCC, the dotted line in Fig. 8 is obtained; the coupling potentials with $\lambda = 2$ are artificially multiplied by 0.7, following the analysis of the MSU data [13]. One sees from Fig. 8 that inclusion of the reduced E2 component somewhat increases the breakup cross section, which gives further decrease of $S_{17}(0)$, i.e. $S_{17}(0) = 17.9_{-1.6}^{+1.7} \text{ eV b}$ is obtained. This result is consistent with the conclusion of Ref. [13], where $S_{17}(0) = 17.8_{-1.2}^{+1.4} \text{ eV b}$ was derived with first-order perturbation theory including both E1 and reduced E2 components. We found that if the E2 component is not scaled in the one-step Coulomb calculation, the resulting value of $S_{17}(0)$ is 16.7 eV b. Since the coupling po-

tentials with $\lambda \geq 3$ are found to little affect the total breakup-cross-section for $\theta_8 \leq 4^\circ$, one sees the higher-order processes increase $S_{17}(0)$ by about 20%, by comparing the value of 16.7 eV b with the result of full CDCC, 20.9 eV b.

Thus, description of ^8B breakup process with both the E1 and E2 transitions and also with higher-order processes is a key to solve a puzzle of $S_{17}(0)$, that is, the discrepancy between the values of $S_{17}(0)$ extracted from direct p -capture reactions and indirect Coulomb-dissociation experiments. In order to clarify the role of these components in more detail, systematic analysis of ^8B breakup reactions with CDCC and the ANC method will be necessary. Analysis of parallel momentum (p_{\parallel}) distribution of ^7Be -fragment after breakup of ^8B is particularly important, since the role of E2 component was determined from that quantity in MSU experiment [12, 13]. It should be remarked that the analysis in Ref. [13] contains CDCC calculation that is essentially the same as in the present paper. However, no quantitative evaluation of the effects of multistep processes was done there. A CDCC analysis of the p_{\parallel} distribution has been done by Mortimer *et al.* [27], where the dependence of the calculated result on the strength of coupling potentials with $\lambda = 2$, which corresponds to E2 transitions. They found that the E2-transition potentials must be multiplied by 1.6 to reproduce the experimental data, although the origin of the enhancement was not clarified. However, their calculation did not concern the resolution and efficiency of the measurement [51]. Thus, it appears that the accuracy of the enhancement-factor 1.6 needs to be further investigated. Unfortunately, filtering-table for the MSU experiment is not available. Thus, at this stage, we can quantitatively extract $S_{17}(0)$ with CDCC and the ANC method only from the ^8B breakup experiment done at RIKEN. Nevertheless, comparison of our pure theoretical result with that shown in Ref. [27] is very interesting, which will be reported in future.

E. ANC analysis of the direct measurement

We have also applied the ANC method to the direct p -capture reaction $^7\text{Be}(p, \gamma)^8\text{B}$ at energies of 116–362 keV [4], with assuming a simple potential-model of ^8B . We calculated the matrix elements of the pure E1-transitions of p and ^7Be to the final state, i.e. the ground state of ^8B , including the s - and d -state components of the initial wave-function of p - ^7Be . We use the same single-particle potential for the bound and scattering states of ^8B as in Sec. III A. The intrinsic spins of p and ^7Be are explicitly included by adopting the channel-spin representation, just in the same way as in the calculation of ^8B breakup. In Fig. 9 the solid line shows the calculated S_{17} as a function of the c.m. energy $E_{c.m.}$ of p - ^7Be in the initial state. The plotted $S_{17}(E)$ has been multiplied by the spectroscopic factor $\mathfrak{S}_{\text{exp}} = 1.15$, which is the result of the χ^2 -fit using the data below 362 keV. Obviously the calculated $S_{17}(E)$ is not reliable in high-energy region, say $E_{c.m.} > 400$ keV, where the inner part of the ^8B wave function plays an important role. In contrast to that, at low energies, the ANC method works very well and a reliable value of the ANC C , or $S_{17}(0)$, can be derived from the χ^2 -fitting procedure. The resulting value

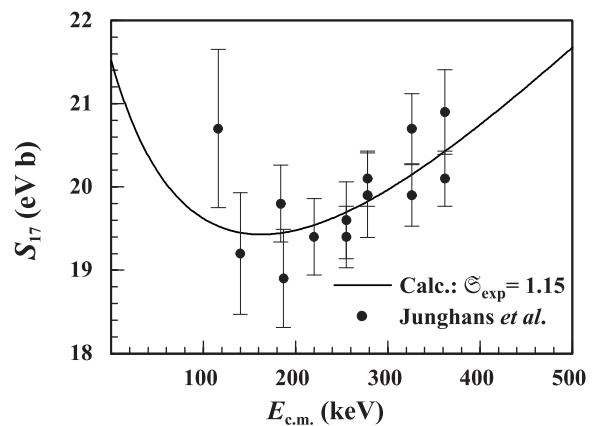


FIG. 9: The astrophysical factor S_{17} as a function of the c.m. energy of p - ^7Be . The solid line is the result of the calculation with a simple potential model, multiplied by $\mathfrak{S}_{\text{exp}} = 1.15$. The experimental data are taken from Ref. [4].

of $S_{17}(0)$ is 21.7 eV b. Uncertainties of the $S_{17}(0)$ are evaluated just in the same way as in Sec. III C and found to be $+0.37/-0.24$ eV b, almost all of which is due to the ambiguity of the s -state potentials for the $S = 1$ and $S = 2$ channels of p - ^7Be . By adding the 2.3% systematic experimental error to the theoretical one in quadrature, we obtain the following result: $S_{17}(0) = 21.7_{-0.55}^{+0.62}$ eV b. This result is consistent with both the extracted $S_{17}(0)$ from ^8B dissociation in the present paper, $S_{17}(0) = 20.9_{-0.6}^{+1.0}$ (theo) ± 1.8 (expt) eV b, and the result obtained in Ref. [4], $S_{17}(0) = 22.1 \pm 0.6$ (expt) ± 0.6 (theo) eV b. It should be remarked that in the present ANC analysis the uncertainty of $S_{17}(0)$ concerning with the ambiguous p - ^7Be scattering-length is directly evaluated, in contrast to the analysis in Ref. [4].

IV. SUMMARY

The astrophysical factor $S_{17}(0)$ for $^7\text{Be}(p, \gamma)^8\text{B}$ is determined from $^{208}\text{Pb}(^8\text{B}, p+^7\text{Be})^{208}\text{Pb}$ at 52 MeV/nucleon measured at RIKEN, by using the asymptotic normalization coefficient (ANC) method. We show the ^8B breakup cross section calculated with the method of continuum-discretized coupled-channels (CDCC) is indeed proportional to the spectroscopic factor $\mathfrak{S}_{\text{exp}}$ as long as the ^7Be core is not excited during the breakup process of ^8B . This condition is satisfied for forward scattering of ^8B below about 4° . In the calculation of CDCC, the scattering amplitude corresponding to large values of orbital-angular-momentum is obtained by the eikonal-CDCC method (E-CDCC) to make an efficient analysis. We have improved the formulation of E-CDCC on the treatment of the Coulomb wave function and that of the intrinsic spin of the projectile. The calculated angular distribution of the breakup cross section, after taking account of the resolution and efficiency for the experiment, well reproduces the measured one at forward angles and underestimates it at backward angles. The underestimation is possibly due to the lack of the

resonance structure of ${}^8\text{B}$ or neglect of the dynamical contribution of the excited-core component of ${}^8\text{B}$ in the present analysis.

The value of the ANC is extracted by comparing the theoretical breakup-cross-section with the experimental data below 4° and $S_{17}(0) = 20.9$ eV b is obtained. The uncertainty of the $S_{17}(0)$ coming from the use of the ANC method and that from the ambiguity of the distorting potentials are both found to be negligible. On the contrary, the uncertainty of the s-state single-particle potentials of ${}^8\text{B}$ for the $S = 1$ and $S = 2$ channels brings the $+4.5\%/ -2.6\%$ error of $S_{17}(0)$. Thus, as the main result of the present paper, $S_{17}(0) = 20.9^{+1.0}_{-0.6}$ (theo) ± 1.8 (expt) eV b is obtained, which is consistent with the result derived from the precise direct measurement of ${}^7\text{Be}(p, \gamma){}^8\text{B}$: $S_{17}(0) = 22.1 \pm 0.6$ (expt) ± 0.6 (theo) eV b.

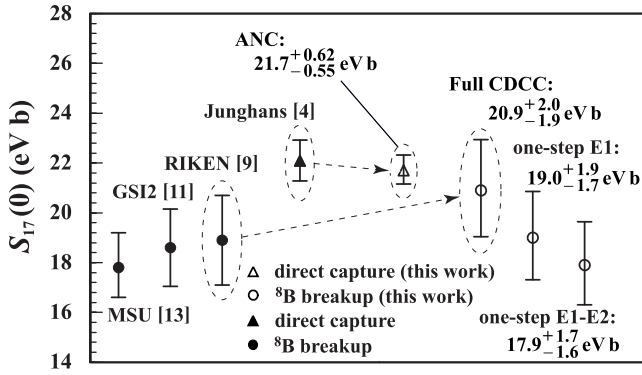


FIG. 10: The results of $S_{17}(0)$ extracted by the ANC method are shown by open symbols: the circles are obtained from three-types of CDCC analysis of ${}^8\text{B}$ breakup and the triangle is the result of analysis of ${}^7\text{Be}(p, \gamma){}^8\text{B}$ with a simple potential model. The result of $S_{17}(0)$ determined by the precise direct measurement [4] (closed triangle) and those obtained from ${}^8\text{B}$ dissociation with first-order perturbation theory (closed circles) are also shown for comparison.

We show that if the one-step Coulomb dipole (E1) transi-

tions of ${}^8\text{B}$ is assumed to describe ${}^8\text{B}$ breakup, the resulting $S_{17}(0)$ is $19.0^{+1.9}_{-1.7}$ eV b, i.e. about 9% decrease of $S_{17}(0)$ is found; this value is quite close to the result of $S_{17}(0) = 18.9 \pm 1.8$ eV b determined from the same experiment by using the first-order perturbation theory. The inclusion of the Coulomb quadrupole (E2) transitions, scaled by 0.7, in the one-step calculation is found to further decrease $S_{17}(0)$ by about 6%, i.e. $S_{17}(0) = 17.9^{+1.7}_{-1.6}$ eV b is obtained. Multistep processes are found to make $S_{17}(0)$ increase by about 20%. Consequently, the present analysis shows the importance of the description of ${}^8\text{B}$ breakup process with both the E1 and E2 transitions and also with higher-order processes. In order to draw a definite conclusion on the role of E2 transitions, however, intensive analysis of the parallel momentum distribution of ${}^7\text{Be}$ -fragment after breakup of ${}^8\text{B}$, carefully taking account of experimental resolution and efficiency, will be necessary. The ANC method is also applied to direct measurement of ${}^7\text{Be}(p, \gamma){}^8\text{B}$ at energies from 116 keV to 362 keV and $S_{17}(0) = 21.7^{+0.62}_{-0.55}$ eV b is obtained, which is consistent with the result of the recent precise measurement of $S_{17}(0)$, i.e. $S_{17}(0) = 22.1 \pm 0.6$ (expt) ± 0.6 (theo) eV b.

In conclusion, the agreement between the values of $S_{17}(0)$ derived from direct (p, γ) and indirect ${}^8\text{B}$ -breakup measurements is significantly improved, as shown in Fig. 10. Accurate description of the ${}^8\text{B}$ breakup process by CDCC, with E1 and E2 transitions and all higher-order processes, is of crucial importance to derive a reliable value of $S_{17}(0)$. Our main result of $S_{17}(0)$ obtained from ${}^{208}\text{Pb}({}^8\text{B}, p+{}^7\text{Be}){}^{208}\text{Pb}$ at 52 MeV/nucleon is $S_{17}(0) = 20.9^{+2.0}_{-1.9}$ eV b.

Acknowledgments

The authors would like to thank T. Motobayashi for helpful discussions and providing detailed information on the experiment. The authors also thank M. Kawai for fruitful discussions. This work has been supported in part by the Grants-in-Aid for Scientific Research of Monbukagakusyou of Japan.

-
- [1] J. N. Bahcall, M. H. Pinsonneault and Sarbani Basu, *Astrophys. J.* **555**, 990 (2001) and references therein.
 - [2] J. N. Bahcall, M. C. Gonzalez-Garcia and Carlos Peña-Garay, *JHEP* **0108**, 014 (2001) [arXiv:hep-ph/0106258]; *JHEP* **0302**, 009 (2003) [arXiv:hep-ph/0212147].
 - [3] J. N. Bahcall, *Nucl. Phys. B Proc. Suppl.* **118**, 77 (2003).
 - [4] A. R. Junghans *et al.*, *Phys. Rev. C* **68**, 065803 (2003).
 - [5] P. Descouvemont and D. Baye, *Nucl. Phys. A* **567**, 341 (1994).
 - [6] P. Descouvemont, *Phys. Rev. C* **70**, 065802 (2004).
 - [7] T. Motobayashi *et al.*, *Phys. Rev. Lett.* **73**, 2680 (1994);
 - [8] T. Kikuchi *et al.*, *Phys. Lett. B* **391**, 261 (1997).
 - [9] T. Kikuchi *et al.*, *Eur. Phys. J. A* **3**, 209 (1998).
 - [10] N. Iwasa *et al.*, *Phys. Rev. Lett.* **83**, 2910 (1999).
 - [11] F. Schümann *et al.*, *Phys. Rev. Lett.* **90**, 232501 (2003).
 - [12] B. Davids *et al.*, *Phys. Rev. Lett.* **86**, 2750 (2001).
 - [13] B. Davids *et al.*, *Phys. Rev. C* **63**, 065806 (2001).
 - [14] H. Esbensen, G. F. Bertsch and K. A. Snover, *Phys. Rev. Lett.* **94**, 042502 (2005).
 - [15] M. Kamimura *et al.*, *Prog. Theor. Phys. Suppl.* **89**, 1 (1986).
 - [16] N. Austern *et al.*, *Phys. Reports.* **154**, 125 (1987).
 - [17] M. Yahiro, M. Nakano, Y. Iseri and M. Kamimura, *Prog. Theor. Phys.* **67**, 1467 (1982).
 - [18] M. Yahiro, Y. Iseri, M. Kamimura and M. Nakano, *Phys. Lett.* **141B**, 19 (1984).
 - [19] Y. Sakuragi and M. Kamimura, *Phys. Lett.* **149B**, 307 (1984).
 - [20] Y. Sakuragi, *Phys. Rev. C* **35**, 2161 (1987).
 - [21] Y. Sakuragi, M. Kamimura and K. Katori, *Phys. Lett.* **B205**, 204 (1988); Y. Sakuragi, Y. Yahiro, M. Kamimura and M. Tanifuji, *Nucl. Phys.* **A480**, 361 (1988).
 - [22] Y. Iseri, H. Kameyama, M. Kamimura, M. Yahiro and M. Tanifuji, *Nucl. Phys.* **A490**, 383 (1988).
 - [23] Y. Hirabayashi and Y. Sakuragi, *Phys. Rev. Lett.* **69**, 1892

- (1992).
- [24] J. A. Tostevin *et al.*, Phys. Rev. C **66**, 024607 (2002); A. M. Moro, R. Crespo, F. Nunes and I. J. Thompson, Phys. Rev. C **66**, 024612 (2002) and references therein.
- [25] K. Ogata, M. Yahiro, Y. Iseri and M. Kamimura, Phys. Rev. C **67**, 011602(R) (2003).
- [26] J. A. Tostevin, F. M. Nunes and I. J. Thompson, Phys. Rev. C **63**, 024617 (2001).
- [27] J. Mortimer, I. J. Thompson and J. A. Tostevin, Phys. Rev. C **65**, 064619 (2002).
- [28] K. Ogata *et al.*, Nucl. Phys. A **738c**, 421 (2004).
- [29] A. M. Mukhamedzhanov and N. K. Timofeyuk, Yad. Fiz. **51**, 679 (1990) [Sov. J. Nucl. Phys. **51**, 431 (1990)].
- [30] H. M. Xu, C. A. Gagliardi, R. E. Tribble, A. M. Mukhamedzhanov and N. K. Timofeyuk, Phys. Rev. Lett. **73**, 2027 (1994).
- [31] K. Ogata, M. Yahiro, Y. Iseri, T. Matsumoto and M. Kamimura, Phys. Rev. C **68**, 064609 (2003).
- [32] D. Baye, Phys. Rev. C **62**, 065803 (2000).
- [33] A. Azhari *et al.*, Phys. Rev. Lett. **82**, 3960 (1999).
- [34] A. Azhari *et al.*, Phys. Rev. C **60**, 055803 (1999).
- [35] Y. Iseri, M. Yahiro and M. Kamimura, Prog. Theor. Phys. Suppl. **89**, 84 (1986).
- [36] N. Austern, M. Yahiro and M. Kawai, Phys. Rev. Lett. **63**, 2649(1989); N. Austern, M. Kawai and M. Yahiro, Phys. Rev. C **53**, 314 (1996).
- [37] M. Yahiro and M. Kamimura, Prog. Theor. Phys. **65**, 2046 (1981); **65**, 2051 (1981).
- [38] T. Matsumoto *et al.*, Phys. Rev. C **68**, 064607 (2003).
- [39] A. M. Moro *et al.*, Phys. Rev. C **65**, 011602(R) (2001).
- [40] R. Y. Rasoanaivo and G. H. Rawitscher, Phys. Rev. C **39**, 1709 (1989).
- [41] M. Kawai, private communication (2003).
- [42] See, for example, Y. Watanabe *et al.*, Phys. Rev. C **59**, 2136 (1999).
- [43] H. Esbensen and G. F. Bertsch, Nucl. Phys. A **600**, 66 (1996).
- [44] F. C. Barker, Aust. J. Phys. **33**, 177 (1980).
- [45] C. Angulo *et al.*, Nucl. Phys. A **716**, 211 (2003).
- [46] A. J. Koning and J. P. Delaroche, Nucl. Phys. A **713**, 231 (2003).
- [47] J. Cook, Nucl. Phys. A **388**, 153 (1982).
- [48] T. Motobayashi, private communication (2004).
- [49] K. H. Kim, M. H. Park and B. T. Kim, Phys. Rev. C **35**, 363 (1987).
- [50] I. Tanihata *et al.*, Phys. Rev. Lett. **55**, 2676 (1985).
- [51] F. M. Nunes, private communication (2005).